Heliyon 10 (2024) e35637

Contents lists available at ScienceDirect

Heliyon

journal homepage: www.cell.com/heliyon

Research article

Impact of prenatal THC exposure on lipid metabolism and microbiota composition in rat offspring

Elisabetta Murru [a,2], Gianfranca Carta [a,2], Claudia Manca [a,2], Marko Verce [b,c], Amandine Everard [b,c], Valeria Serra [a], Sonia Aroni [a], Miriam Melis [a,1], Sebastiano Banni [a,*,1]

[a] Department of Biomedical Sciences, University of Cagliari, 09042, Monserrato, Italy
[b] Metabolism and Nutrition Research Group, Louvain Drug Research Institute, UCLouvain, Université catholique de Louvain, Brussels, Belgium
[c] Walloon Excellence in Life Sciences and BIOtechnology (WELBIO) department, WEL Research Institute (WELRI), avenue Pasteur, 6, 1300, Wavre, Belgium

A B S T R A C T

Objective: Recent studies have demonstrated that prenatal exposure to the psychoactive ingredient of cannabis that is tetrahydrocannabinol (THC) disrupts fatty acid (FA) signaling pathways in the developing brain, potentially linking to psychopathologic consequences. Our research aims to investigate whether changes in midbrain FA metabolism are linked to modifications in peripheral metabolism of FAs and shifts in microbiota composition.

Methods: In order to model prenatal exposure to THC (PTE) in rats, Sprague Dawley dams were systemically administered with THC (2 mg/kg, s.c.) or vehicle once daily from gestational day 5–20. To evaluate the metabolic impact of PTE in the offspring during preadolescence (postnatal day, PND, 25–28), we analyzed FA profiles and their bioactive metabolites in liver and midbrain tissues, and microbiota alterations.

Results: Our findings indicate that PTE leads to sex-specific metabolic changes. In both sexes, PTE resulted in increased liver de novo lipogenesis (DNL) and alterations in FA profiles, as well as changes in N-acylethanolamines (NAEs), ligands of peroxisome proliferator-activated receptor alpha (PPAR-α). In females only, PTE influenced gene expression of PPAR-α and fibroblast growth factor 21 (Fgf21). In male offspring only, PTE was associated with significantly reduced fasting glycaemia and with alterations in the levels of midbrain NAEs. Our analysis of the progeny gut microbiota revealed sex-dependent effects of PTE, notably an increased abundance of *Ileibacterium* in PTE-exposed male offspring, a change previously associated with the long-term effects of a maternal unbalanced diet.

Conclusions: Our data suggest that in male PTE offspring a reduced fasting glycaemia, resulting from increased liver DNL and the absence of a compensatory effect by *Ppar-α* and *FGF21* on glycemic homeostasis, are associated to alterations in midbrain NAEs ligands of PPAR-α. These metabolic changes within the midbrain, along with *Ileibacterium* abundance, may partly elucidate the heightened susceptibility to psychopathologic conditions previously observed in male offspring following PTE.

1. Introduction

The use of cannabinoids during pregnancy for the relief of nausea, anxiety, and other pregnancy-related conditions is increasing [1] and so is the growing perception and belief that cannabis derivatives could serve as a natural therapeutic remedy even during such a sensitive window of development [2,3]. However, emerging evidence suggests that prenatal cannabis exposure, particularly to its main

* Corresponding author. Department of Biomedical Sciences, University of Cagliari, 09042 Monserrato, Cagliari, Italy.
E-mail address: banni@unica.it (S. Banni).
[1] These Authors share co-seniorship.
[2] These Authors have contributed equally to this work.

https://doi.org/10.1016/j.heliyon.2024.e35637
Received 8 January 2024; Received in revised form 31 July 2024; Accepted 1 August 2024
Available online 2 August 2024

psychotropic component Δ9-tetrahydrocannabinol (THC), which crosses the placenta and impacts fetus development, increases the risk of psychopathology, including psychotic-like events, depression, anxiety, and sleep disorders in children and later in life [4,5]. Prenatal THC exposure (PTE) leads to adverse morphological changes in placenta with reduced glucose transporter 1 (GLUT1) and glucocorticoid receptor expression [6,7]. These effects implicate impaired maternal-to-fetal glucose transport that has been associated to low birth weight and fetal growth restriction, including decreased head circumference [8,9].

In rats, PTE has been shown to interfere with fatty acid (FA) signaling pathways in the developing brain, directly in the mesolimbic circuitry, which could potentially be associated with several pathophysiological outcomes [10]. Particularly, female offspring exhibited more significant alterations in FA levels during prepubescence but appeared to recover from these deficits in early adulthood. In contrast, PTE male offspring consistently displayed deficits in FA metabolic pathways into adulthood. Moreover, PTE progeny displayed lasting abnormalities in glutamatergic/GABAergic function in brain (i.e., nucleus accumbens). These findings revealed several new long-term risks of maternal cannabis use and, for the first time, demonstrated sex-related effects of maternal cannabinoid exposure directly on the developing neural lipidome [10].

PTE has also been linked to peripheral metabolic imbalances potentially contributing to the development of metabolic syndrome. An association between fetal exposure to cannabis and increased adiposity and fasting glucose levels in early childhood has been suggested [11]. Fetal exposure to cannabis may disrupt molecular control of insulin and glucagon release [12]. Notably, these metabolic changes might be ascribed to impaired FA metabolism and may lead to metabolic syndrome [13]. Indeed, FAs may play distinct roles in regulating inflammatory signals and insulin resistance (IR) [14].

IR can impair glycogen synthesis in the liver, thereby triggering de novo lipogenesis (DNL), a process aimed at managing excessive glucose accumulation by converting it into FAs, mainly palmitic acid (16:0, PA) and its metabolites, namely palmitoleic (16:1, POA) and oleic (18:1, OA) acids [15]. These latter may be transported from the liver to the bloodstream via VLDL, resulting in higher tissue deposition of PA. Over time, this could initiate an abnormal systemic inflammatory response and a metabolic dysregulation, potentially resulting in dyslipidemia, IR, altered fat deposition, and other pathological conditions [16].

In addition, it has been well established that CB1 activation induces de novo lipogenesis (DNL) [17].

Notably, gut microbes and bioactive metabolites related to the endocannabinoidome (eCBome) have also been identified as important factors modulating systemic inflammation, IR and fat accumulation [18].

Despite this compelling evidence, how PTE affects FA metabolism in peripheral tissues in the rat offspring, and how this impacts the production of bioactive metabolites associated with the eCBome, and the gut microbiota is an understudied subject. This knowledge is highly relevant because changes in tissue FA profile, especially those esterified to phospholipids acting as precursors, can significantly influence the biosynthesis of bioactive metabolites belonging to the eCBome [19,20]. These metabolites have the potential to regulate lipid and energy metabolism by affecting the peroxisome proliferator-activated receptor alpha (PPAR-α) and the endocannabinoid (eCB) systems [21–23]. Equally important, augmented DNL may exert multifaceted effects on both PPAR-α and eCB systems, by enhancing FA biosynthesis, which both directly and/or through intermediary metabolites act as ligands for both systems [16,24]. Lastly, changes in FA metabolism may alter gut microbiota composition as an additional adaptive homeostatic mechanism [25].

The objective of our study is to explore the interrelation between prenatal THC exposure and its subsequent effects on peripheral FA metabolism and the variation of gut microbiota particularly considering the differences between sexes. Additionally, we aim to elucidate how these variables collectively impact FA metabolism within the midbrain. By doing so, we intend to provide a deeper understanding of the pathophysiological outcomes previously observed as a result of PTE.

2. Materials and methods

2.1. Experimental design

All experimental procedures were carried out according to the European legislation EU Directive 2010/63 and were approved by the Animal Ethics Committees of the University of Cagliari and by Italian Ministry of Health (auth. No. 256/2020). We made all efforts to minimize pain and suffering and to reduce the number of animals used. Primiparous female Sprague Dawley rats (Envigo) were used as mothers and single-housed during pregnancy. Offspring were weaned at postnatal day (PND) 21 and were housed in a climate-controlled animal room (21 ± 1 °C; 60 % humidity) under a normal 12 h light–dark cycle (lights on at 7:00 a.m.) with ab libitum access to water and food.

All the experiments were conducted in both sexes during preadolescence (PND25–28). All animals included in this study did not undergo any pharmacological manipulation during their postnatal life.

THC resin was purchased from THC PHARM GmbH (Frankfurt, Germany) and dissolved in ethanol at 20 % final concentration. Then, THC was suspended in a vehicle (VEH) solution containing 1–2% Tween® 80 and diluted with sterile saline (0.9 % NaCl).

To model PTE, rat dams were administered subcutaneously (s.c.) with THC (2 mg/kg, 2 mL kg^{-1}) or VEH once per day from GD5 until GD20. This dose of THC was chosen because it does not elicit substantial behavioral responses or tolerance after repeated administration [26]. Moreover, it fails to affect maternal or non-maternal behavior, or offspring litter size [27]. Notably, this dose of THC is equivalent to the current estimates of moderate cannabis consumption in humans since it is similar to the THC content in mild joints (5 %) [28].

2.2. Fatty acid analysis

Total lipids were extracted from liver, plasma and midbrain samples according to the method of Folch [29]. Total lipid

quantification was performed by the method of Chiang [30]. Aliquots of the lipid fraction were mildly saponified in order to obtain free FAs (FFA) [31] for High Performance Liquid Chromatograph (HPLC) and Gas Chromatograph (GC) analysis. The separation and identification of UFA was carried out using an Agilent 1100 HPLC System (Agilent, Palo Alto, CA, USA) equipped with a diode array detector (DAD) as previously reported [29]. SFAs were measured as FA methyl esters (FAME) by a GC (Agilent, Model 6890, Palo Alto) equipped with a flame ionization detector (FID) [32].

2.3. NAEs and 2-MG analysis

Deuterated N-acylethanolamine (NAEs) and congeners were added as internal standards to the samples before extraction for quantification by isotope dilution, aliquots of the lipid fraction were used for their quantification. Internal deuterated standards N-arachidonoylethanolamine $[2H]_8$AEA, N-oleoylethanolamine $[2H]_2$OEA, N-palmitoylethanolamine $[2H]_4$PEA, N-stearoylethanolamine $[2H]_3$SEA, 2-arachidonoyl-glycerol-d5 $[2H]_5$2AG were purchased from Cayman Chemicals (MI, USA). NAEs quantification was carried out by an Agilent 1260 UHPLC system (Agilent, Palo Alto) equipped with a mass spectrometry (MS) Agilent Technologies QQQ triple quadrupole 6420 with electrospray ionization (ESI) source, using positive mode (ESI+) as described in Manca et al. [33].

2.4. Glycaemia

The glycaemia measurement in whole blood was carried out with medical devices GlucoMen areo meter and GlucoMen areo Sensor (A. Menarini Diagnostics Srl, Italy). The test range of sensors is 20–600 mg/dL.

2.5. RNA isolation, reverse transcription and qPCR-based TaqMan open array

RNA was extracted from liver samples by TRI Reagent solution (Thermo Fisher Scientific, MA, USA) following the manufacturer's instruction and eluted in 100 μl of UltraPure Distilled Water (Invitrogen, CA, USA). The concentration and purity of RNA were determined by measuring the absorbance of the RNA in a Biodrop at 260 nm and 280 nm, and RNA integrity was assessed using Agilent Tapestation 4200 System (Agilent Technologies, CA, USA). 1 μg of total RNA was reverse transcribed using the High-Capacity cDNA Reverse Transcription Kit (Thermo Fisher Scientific, MA, USA) in a reaction volume of 20 μl. 10 ng of starting RNA were used to evaluate the expression of *Ppar-α* and fibroblast growth factor 21 (*Fgf21*) using specific forward and reverse primer pairs (Biorad, CA, USA) on a Rotorgene Q System (Biorad, CA, USA) using PowerUp SYBR Green qPCR master mix (Thermo Fisher Scientific, CA, USA) in duplicate reactions. TATA box binding protein (*Tbp*) was used as reference gene. Gene expression levels were evaluated by the $2^{-\Delta\Delta Ct}$ method and represented as fold increase with respect to baseline.

2.6. Statistical analysis

Statistical analysis was conducted using GraphPad Prism 8.0.1 software (La Jolla, CA, USA). The ROUT method and Shapiro-Wilk normality test were employed to identify and remove any outliers and to assess the normal distribution of the data, respectively. As the data did not follow normal distribution, for each sex, non-parametric Mann-Whitney tests were performed to evaluate differences between PTE and CTRL group.

Results are presented as mean ± standard deviation, and a significance level of $p \leq 0.05$ was used to determine statistical significance among the groups.

2.7. Microbiome

2.7.1. DNA isolation from rat caecal samples and sequencing

DNA was isolated from the caecal content of the offspring using the DNeasy PowerSoil Pro kit (Qiagen, Hilden, Germany) following the manufacturers' instructions. After the assessment of concentration by using DeNovix DS-11 nanospectrophotometer and DeNovix QFX fluorometer technologies (DeNovix, DE, USA), DNA was used as template for the amplification of the V3–V4 region of the 16S rRNA gene by using specific primers 5′-CCTACGGGNGGCWGCAG-3′ and 5′-GGACTACHVGGGTATCTAATCC-3' (Integrated DNA Technologies IDT, IA, USA) and KAPA HiFi HotStart ReadyMix (Roche) in conjunction with the Nextera XT Index Kit v2 (Sets A and B) kit (Illumina, CA, USA). The expected amplicon size was approximately 600 base pairs, confirmed using the Agilent Tapestation 4200 System (Agilent, CA, USA). Libraries were normalized, pooled to 4 nM, then denatured, and diluted to a final concentration of 10pM, supplemented with 20 % PhiX control (Illumina, CA, USA). Sequencing (2 × 300 bp paired-end) was performed using the MiSeq Reagent Kit V3 (600 cycles) on an Illumina MiSeq System.

QIIME2 was used to process the resulting data (q2cli 2021.4.0, [34]). Primers were removed with Cutadapt [35], using the following parameters: overlap = 5, error rate = 0.15, discard untrimmed reads. To ensure the quality of the analysis, only the forward reads were used. Reads were denoised with DADA2 [36], using the following parameters: maximum expected errors = 5, truncation length = 252 nt, minimum fold parent over abundance = 4. The resulting amplicon sequence variant (ASV) table was decontaminated by removing the ASVs that mapped to the rat genome mRatBN7.2 (GCF_015227675.2) using BLAST within QIIME2, putative non-16S ASVs left as "Unassigned" after the taxonomy assignment, artefacts resulting from intra-16S mispriming or chimerism, or that were assigned to a taxon that cannot grow in the gut microbiota and was likely a contaminant (order *Thermomicrobiales*). This resulted in 6072 ASVs in 51 samples in total. For taxonomic assignment, a classifier for the V3–V4 region was built using the SILVA 138.1 SSURef

NR99 database [33], dereplicated and trimmed accordingly using RESCRIPt [37]. The 51 samples consisted of between 1 and 329910 sequence reads, with the median and mean number of sequence reads of 98398 and 101631, respectively. Removal of low-quality samples for statistical analyses is described below. The collection of R packages "tidyverse" was used for taxonomic composition visualisation. The sequencing data were submitted to the European Nucleotide Archive (ENA/EBI) and are available under the study accession number PRJEB71402.

2.8. Microbiome statistical analysis

QIIME2 was used to calculate diversity metrics of the gut microbiota. Using the rarefaction curves, the minimum sample size of 64413 reads was selected. Therefore, 9 samples were excluded from the analysis, resulting in a set of 42 samples with a median and mean of 108873 and 123112, respectively. Weighted and unweighted UniFrac distances [38] were used for the principal coordinate analysis (PCoA) within QIIME2. The corresponding plots were created using the collection of R packages "tidyverse". Differences in alpha-diversity metrics (Pielou's evenness, Faith's phylogenetic diversity) between groups were assessed using the Kruskal-Wallis test and Dunn's test, followed by the Benjamini-Hochberg procedure for all within-sex comparisons and between-sex comparisons of matched groups. Differences in beta-diversity metrics were assessed using Adonis, PERMANOVA, and PERMDISP with 9999 permutations within QIIME2. The adjusted p-values were obtained using the Benjamini-Hochberg procedure where applicable and denoted as q. ANCOM [39] was used as a compositional data analysis tool to find differentially abundant ASVs.

3. Results

To assess the systemic metabolic effects of PTE, we analyzed the profiles of FAs and their bioactive metabolites associated with the

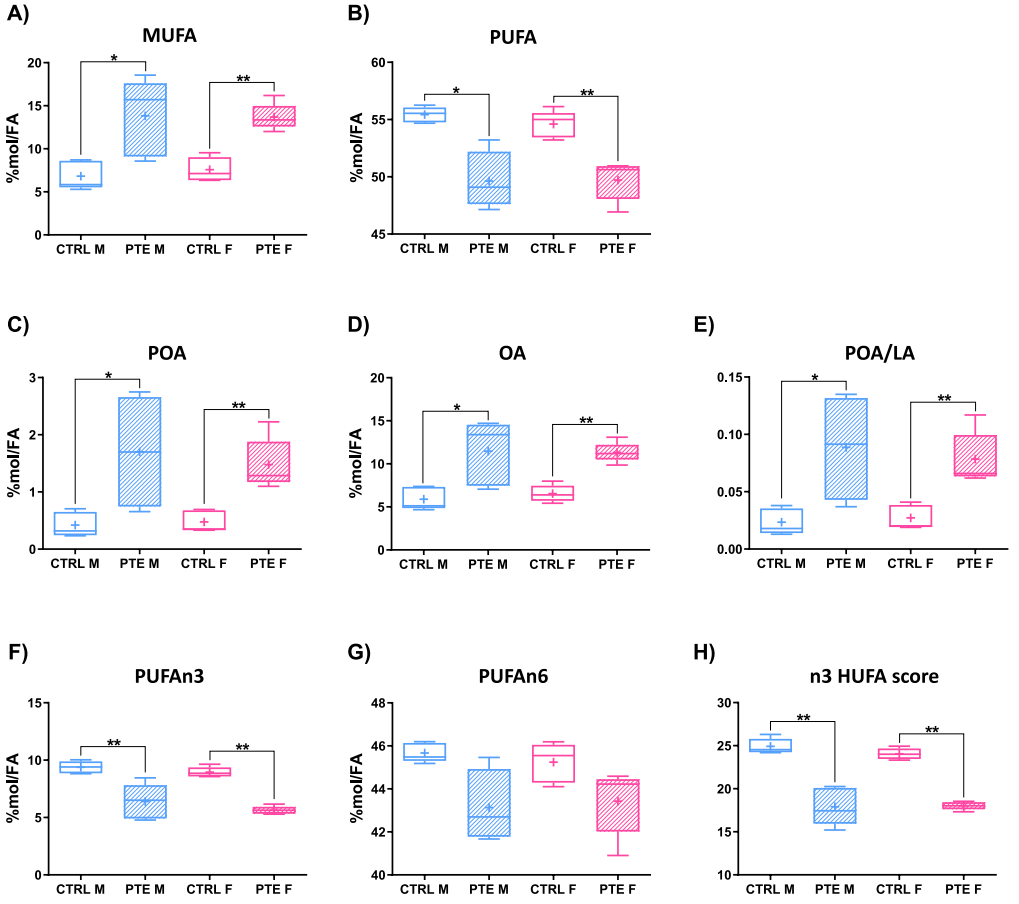

Fig. 1. A) Monounsaturated Fatty Acids (MUFA), B) Polyunsaturated Fatty Acids (PUFA), C) palmitoleic acid (POA), D) oleic acid (OA) expressed as mol% of total FA, E) POA/OA ratio, F) PUFAn3, G) PUFAn6, as mol% of total FA, and C) n3 highly unsaturated fatty acids (HUFA) score (ratio of n3 HUFA to total n6 + n3 HUFA) in liver of male (blue) and female (red) rat offspring prenatally THC exposed (PTE) and controls (CTRL). Values are mean ± S.D. of n = 5. * = $p \leq 0.05$; ** = $p \leq 0.01$. (For interpretation of the references to colour in this figure legend, the reader is referred to the Web version of this article.)

eCBome in the liver, plasma, and midbrain, as well as changes in the microbiota.

3.1. Body weight and food intake

No changes in body weight and food intake were detected (data not shown).

3.2. Fatty acid metabolism in the liver

In examining liver FA metabolism, we found a significant increase in monounsaturated FA (MUFA) at the expense of poly-unsaturated FA (PUFA) in PTE progeny (Fig. 1A and B), with no changes in saturated FA levels (data not shown). This shift in MUFA and PUFA balance can be attributed to heightened biosynthesis of specific MUFA suggestive of DNL, especially of POA and OA (Fig. 1C and D). Accordingly, the metabolic marker for DNL that is the ratio between POA, which is primarily endogenously produced through DNL, and linoleic acid (18:2, LA), which solely derives from the diet, sharply increased (Fig. 1E). While such an increase is often associated with a high deposition of fat in the liver [40], we found no differences when total liver lipids were evaluated (data not

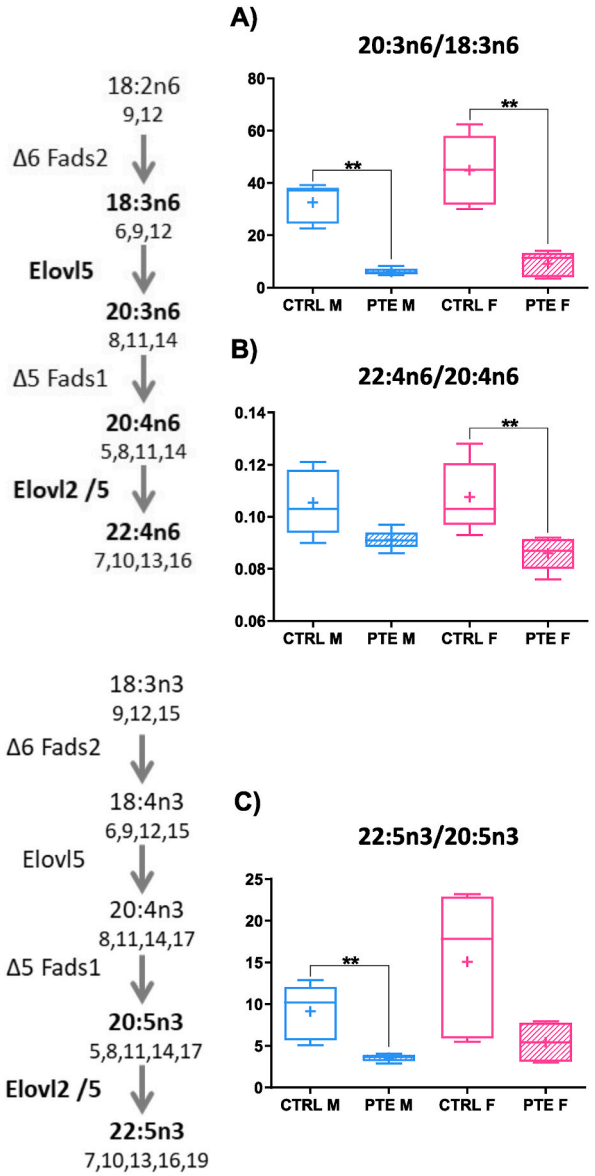

Fig. 2. Prediction of A) Elovl 5 as 20:3n6/18:3n6 ratio, B) Elovl 2/5 as 22:4n6/20:4n6 ratio, C) Elovl 2/5 as 22:5n3/20:5n3 ratio in liver of male (blue) and female (red) rat offspring prenatally THC exposed (PTE) and controls (CTRL). Values are mean ± S.D. of n = 5. ** = $p \leq 0.01$. (For interpretation of the references to colour in this figure legend, the reader is referred to the Web version of this article.)

shown).

A detailed analysis of hepatic PUFA levels shows a reduction in PUFAn3 rather than PUFAn6 (Fig. 1F and G) and suggests the causes for decreased PUFA. Accordingly, the n3 highly unsaturated FA (HUFA) score (ratio of n3 HUFA to total n6 + n3 HUFA), which indicates the tissue n3 and n6 HUFA balance, is markedly reduced (Fig. 1H).

Changes in liver PUFA levels might be ascribed to an altered activity of the elongase 2/5, since PTE progeny exhibited decreased ratios of 20:3n6/18:3n6 and 22:4n6/20:4n6 for the PUFAn6 (Fig. 2A and B) and the diminished ratio of 22:5n3/20:5n3 for the PUFAn3 in the liver (Fig. 2C).

The observed changes in the liver FA profile could influence the biosynthesis of eCB and related compounds, such as NAEs [41]. Accordingly, an increase in NAE levels derived from FAs produced by DNL, such as N-palmitoylethanolamine (PEA), N-palmitoleoylethanolamine (POEA), and N-oleoylethanolamine (OEA), was observed in the PTE progeny (Fig. 3A–C). Of note, the elevated levels of anandamide (AEA) (Fig. 3D) were associated to the decreased n3 HUFA score (Fig. 1H) as previously indicated [41,42]. Conversely, levels of 2-monoacylglycerols (2-MGs) remained unchanged (data not shown).

Considering that PEA, POEA, OEA are potent endogenous ligands for PPAR-α, we further examined if PTE influenced *Ppar-α* gene expression in the liver. Intriguingly, PTE females only displayed increased *Ppar-α* mRNA levels (Fig. 4A). Accordingly, a transcription factor directly regulated by PPAR-α and involved in energy metabolism that is fibroblast growth factor 21 (*Fgf21*) was also enhanced in a sex-dependent fashion (Fig. 4B)

3.3. Lipid and glucose metabolism in the plasma

We further assessed the impact of alterations in hepatic lipid metabolism on plasma glucose and lipid homeostasis. We found a sex-specific reduced glycaemia as a function of PTE (Fig. 5A). Analysis of total plasma FAs (Total FAs) and non-esterified FAs (FFA) revealed a PTE-dependent increase in the progeny (Fig. 5B and C), which was accompanied by a diminished n3 HUFA score (Fig. 5D) and an elevated POA/LA ratio, supportive of the hypothesized increased liver DNL (Fig. 5E).

3.4. Lipid metabolism in the midbrain

We previously found that PTE induced marked alterations in physiological properties and plasticity of midbrain dopamine neurons leading to an abnormally high dopamine cell firing activity [27]. Importantly, this effect was sex-specific and curtailed to the male offspring, thus supporting the existence of sex-dependent mechanisms underlying PTE-induced vulnerability of developing male brains. This prompted us to parse the lipidomic profile of the midbrain. Notably, PTE males only displayed a decreased POA/LA ratio (Fig. 6) and increased levels of PEA and POEA (Fig. 7A–B). Noteworthy, OEA levels rose as a function of PTE irrespective of the sex

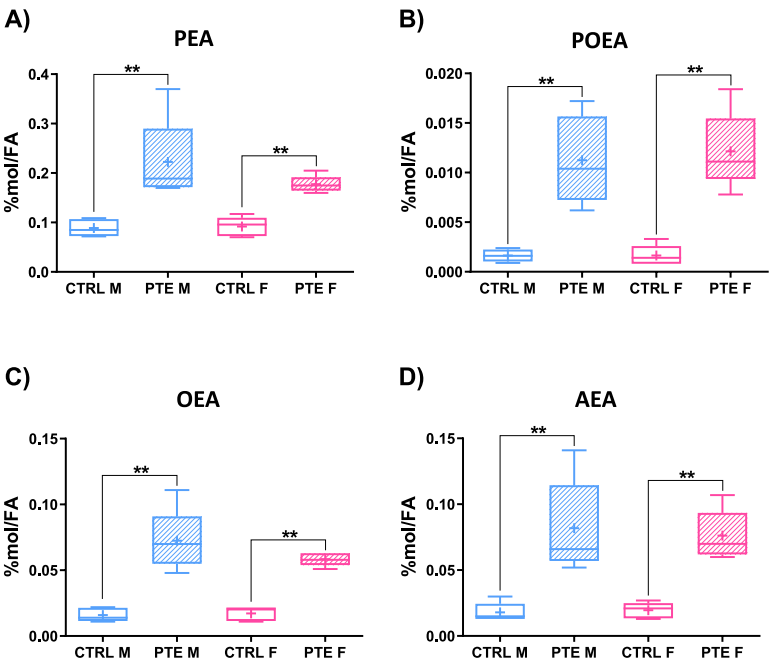

Fig. 3. A) N-palmitoylethanolamine (PEA), B) N-palmitoleoylethanolamine (POEA), C) N-oleoylethanolamine (OEA), and D) anandamide (AEA) as mol% of total FA, in liver of male (blue) and female (red) rat offspring prenatally THC exposed (PTE) and controls (CTRL). Values are mean ± S.D. of n = 5. ** = $p \leq 0.01$. (For interpretation of the references to colour in this figure legend, the reader is referred to the Web version of this article.)

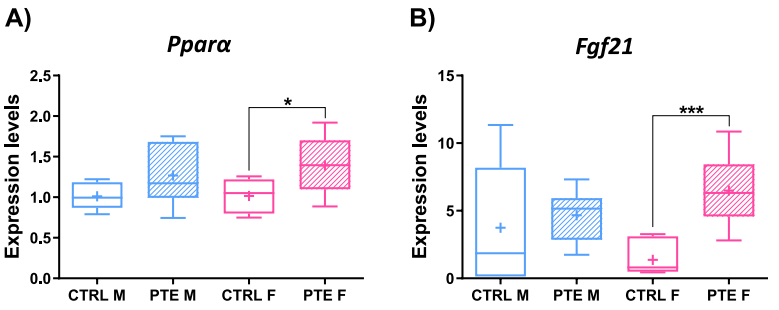

Fig. 4. A) peroxisome proliferator-activated receptor-alpha (*Ppar-α*), B) fibroblast growth factor 21 (*Fgf21*) gene expression in liver of male (blue) and female (red) rat offspring prenatally THC exposed (PTE) and controls (CTRL). Values are mean ± S.D. of n = 5. * = $p \leq 0.05$; *** = $p \leq 0.005$. (For interpretation of the references to colour in this figure legend, the reader is referred to the Web version of this article.)

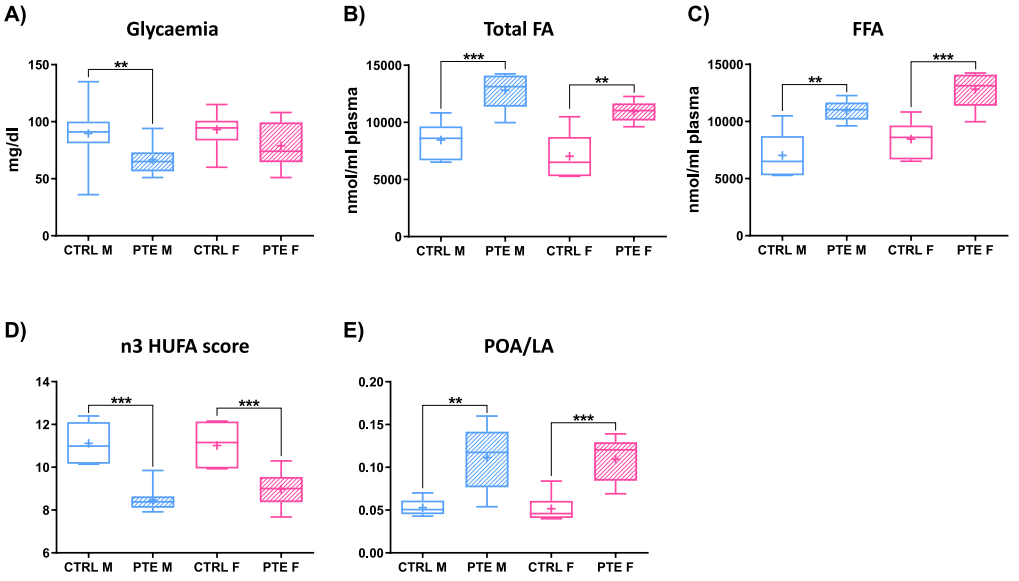

Fig. 5. A) Glycaemia, B) total fatty acid (FA), C) free fatty acids (FFA), D) n3 HUFA score (ratio of highly unsaturated n3 PUFA to total highly unsaturated n6 and n3 PUFAs), E) palmitoleic acid/linoleic acid (POA/LA)) in plasma of male (blue) and female (red) rat offspring prenatally THC exposed (PTE) and controls (CTRL). Values are mean ± S.D. of n = 10 ** = $p \leq 0.01$; *** = $p \leq 0.005$. (For interpretation of the references to colour in this figure legend, the reader is referred to the Web version of this article.)

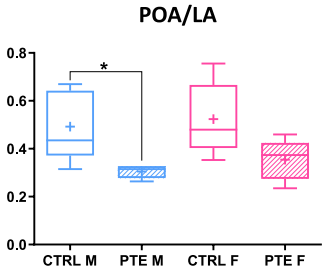

Fig. 6. A) palmitoleic acid/linoleic acid (POA/LA) in midbrain of male (M) and female (F) rat offspring prenatally THC exposed (PTE) and controls (CTRL). Values are mean ± S.D. of n = 5. * = $p \leq 0.05$.

(Fig. 7C). Lastly, PTE did not influence either *Ppar-α* or *Fgf21* gene expression in the midbrain (data not shown).

3.5. Microbiome

3.5.1. Prenatal THC exposure affected the offspring gut microbial composition in a sex-dependent manner

Changes in FA metabolism may alter gut microbiota composition as an additional adaptive homeostatic mechanism [25]. We therefore analyzed the composition of the offspring gut microbiota (Fig. 8A). PTE increased the Shannon index of the gut microbiota of male offspring ($q = 0.0324$; Fig. 8B), representing a combined increase in richness and evenness. However, more specific metrics of gut microbiota evenness, richness, and phylogenetic diversity (Fig. 8C) in males only unveiled a trend towards significance in increased evenness ($q = 0.0526$). This suggests that PTE impacted the relative frequencies of the gut bacteria in males, but not the number of different species or how distinct the species were. Principal component analysis (PCA) shows that PTE also significantly affected microbial community composition, as represented in the PCA plots representing beta-diversity ($p = 0.0001$ and $p = 0.0028$; Fig. 8D and E). The effect of sex was clear when relative frequencies were not considered ($p = 0.0093$ and $p = 0.0467$). This implied sex-dependent differences in low abundant amplicon sequence variants (ASVs) and PTE-dependent differences in more abundant amplicon sequence variant ASVs. Indeed, the ASV-level ANCOM found an increase in two ASVs belonging to *Ileibacterium* and unknown *Actinobacteriota* (likely family *Atopobiaceae*) in PTE male when compared to female progeny. The increased levels of *Ileibacterium* in PTE males were further confirmed at genus level analysis (Fig. 8A). This latter revealed a decrease in [Clostridium] *innocuum* group in the PTE progeny and affected ASVs with a higher relative frequency with a significant decrease in a *Blautia* ASV in PTE females while increasing two *Bifidobacterium* ASVs in PTE males (Fig. 8A). PTE also increased *Gordonibacter* in males (Fig. 8A).

3.6. Discussion

Our results demonstrate that PTE significantly affects lipid metabolism in the liver, which might subsequently influence lipid metabolism in the midbrain. This effect might be driven by the elevated DNL in the liver. This latter might compete for essential acetyl groups with elongases Elovl2 and Elovl5, potentially decreasing PUFA synthesis, particularly n3 PUFA, which could in turn further stimulate DNL [43].

In the liver, DNL typically results from IR, which promotes the accumulation of the newly formed fat from DNL [15]. Conversely, we did not observe increased fat deposition in the liver, possibly because of a prompt fat clearance in the bloodstream through the release of VLDL, as indirectly suggested by the elevated DNL plasmatic biomarker POA/LA. Notably, hepatic DNL correlated with an increase of NAE biosynthesis from the newly synthesized FAs. Concurrently, the heightened n6 to n3 (HUFA) ratio alongside increased NAE biosynthesis can elevate AEA levels, activating type 1-cannabinoid receptors (CB1Rs) that might further stimulate DNL [44].

NAEs such as PEA, POEA, and OEA are potent endogenous ligands of PPARα [45]. Our data identified in the liver a sex-specific augmented gene expression of *Ppar-α* and *Fgf21*, which play a crucial role in energy substrate metabolism [46]. This might suggest that PTE females only might display a heightened sensitivity to endogenous PPARα ligand-induced modulation. Given that PPAR-α and FGF21 have been identified as modulators of glucose homeostasis [46], one might plausibly speculate that their induction in females could counteract the effects of PTE-induced liver FA metabolism disruption on glycaemia homeostasis. Hence, PTE male rats only exhibit a reduced glycaemia at fasting. Of note, PTE male rats also display a decreased DNL and a sustained NAE biosynthesis in the midbrain. One possible explanation could be that the observed reduced glycemia, which may result in decreased glucose availability in the midbrain, might stimulate the production of NAE endogenous PPAR-α ligands. This could promote FA β-oxidation and ketone body formation through PPAR-α activation, thereby addressing the glucose deficit in PTE male rats. Yet, similarly to the liver, the pronounced increase in endogenous PPAR-α ligands did not elevate midbrain *Ppar-α* gene expression in male rats. One might, therefore, speculate that PPAR-α activation can potentially enhance astrocyte metabolism, promoting ketone body production, thus serving as an alternate energy source [47] and conserving glucose essential for the pentose phosphate pathway. This pathway facilitates nucleotide, FA through DNL, and amino acid synthesis, which are critical for synaptogenesis and brain development [48]. Irrespectively, our findings suggest that while PTE male rats might upregulate endogenous PPAR-α ligands in response to decreased glucose availability and DNL, *Ppar-α* gene expression is impaired, thereby impacting their ability to manage glucose deficits within the midbrain. This is

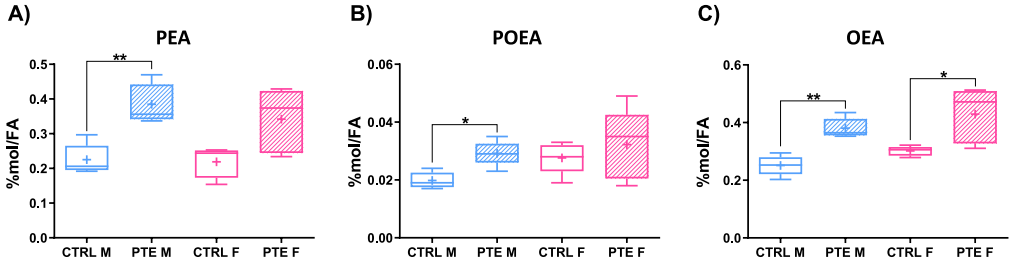

Fig. 7. A) N-palmitoylethanolamine (PEA), B) N-palmitoleoylethanolamine (POEA), and C) N-oleoylethanolamine (OEA), as mol% of total FA, in midbrain of male (M) and female (F) rat offspring prenatally THC exposed (PTE) and controls (CTRL). Values are mean ± S.D. of $n = 5$. * = $p \leq 0.05$; ** = $p \leq 0.01$.

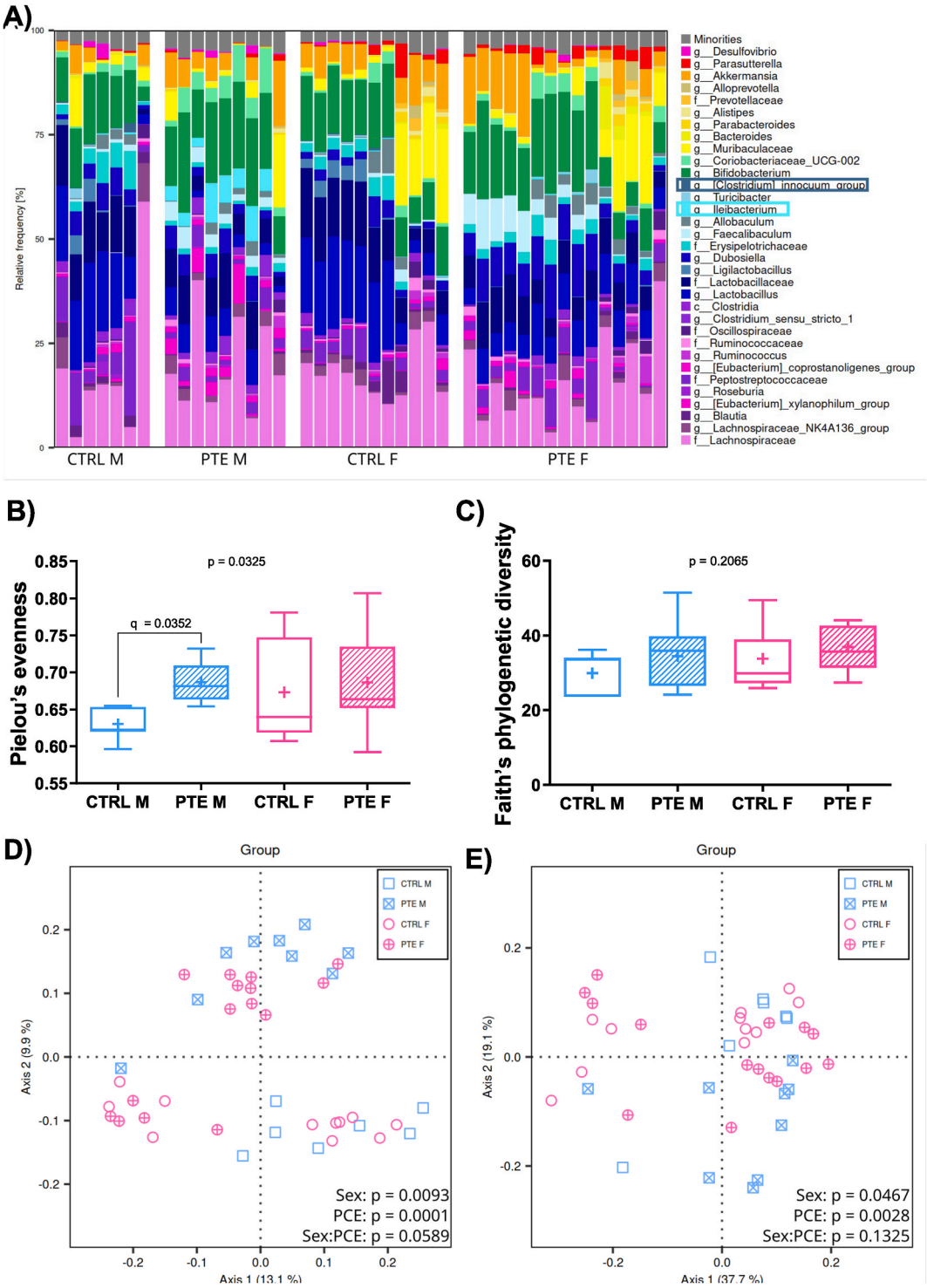

Fig. 8. **(A)** A genus-level taxonomy barplot showing the gut microbiota composition for each sample in all four groups. Amplicon sequence variants (ASVs) assigned to higher taxonomic ranks were grouped accordingly and displayed too. Taxa differentially abundant with statistical significance in at least one comparison are highlighted in the legend. "Minorities" – taxa with <2.0 % relative frequency in all samples. **(B)** Pielou's evenness and **(C)** Faith's phylogenetic diversity for all four groups with Kruskal-Wallis p-values and Dunn's test q-values (FDR-adjusted p-values). **(D)** Principal coordinates analysis plots based on unweighted UniFrac distances and **(E)** weighted UniFrac distances with ADONIS p-values for both factors and their interaction.

relevant because i) neural differentiation occurs throughout life and is strongly associated with upregulation of DNL in neural stem and progenitor cells [49] and ii) DNL is central for the proper morphological formation and function of neurons and for myelination [50].

Our working hypothesis is that during periods of high glucose demand, such as brain development, compensatory homeostatic mechanisms addressing PTE-dependent glucose shortfalls might be insufficient in male rats. These metabolic alterations could be associated with the shifts in the gut microbiome composition. For instance, chronic THC treatment has been suggested to induce hypophagia and to inhibit weight gain in diet-induced obese mice by altering the gut microbiota [51]. Accordingly, we observed a sex dichotomy in PTE effects on the offspring gut microbiota. In particular, *Ileibacterium* abundance is higher in PTE males than females. *Ileibacterium* proliferates in the gut microbiota in high-fat diet or high-fructose and salt diet conditions [52,53]. Notably, offspring exposed in utero to high-fat diet displays an increased risk of neurodevelopmental disorders [54] similar to PTE [4]. *Gordonibacter* increased in PTE males only. *Gordonibacter* abundance has also been observed in gut microbiota of women affected by major depressive disorder [55] and social anxiety disorder [56]. Conversely, in men, *Gordonibacter* is a known producer of anti-inflammatory and neuroprotective urolithins [57,58]. Therefore, the link between the increase in *Gordonibacter* with PTE in males and associated neurologic disorders is less clear. Finally, we observed a reduction in *Blautia* in PTE females relative to their controls that could be associated to IR and DNL. Remarkably, *Blautia* inversely correlated with type 2 diabetes [59]. Collectively, the primary sequence of events suggests that metabolic changes induced by PTE precede and potentially drive alterations in the gut microbiota. These microbiota changes may represent a compensatory mechanism that mitigates the metabolic disturbances initiated by PTE. Specifically, we observed that the increase in certain bacterial species could be interpreted as an adaptive response that restores metabolic balance and counteracts the metabolic dysfunction triggered by PTE.

Furthermore, these microbiota alterations, while secondary to metabolic changes, might contribute to the psychopathological consequences observed in PTE exposure.

Our data suggest that PTE drives significant changes in liver FA metabolism, especially in the induction of DNL. Hepatic metabolic shifts may underlie the alterations observed in other tissues. However, the precise mechanism for such marked impacts on liver metabolism due to PTE remains elusive and warrants further investigations. Previous research has shown that PTE can markedly hinder fetal growth [8,9]. The GLUT1 has been proposed as a potential target for THC, providing an avenue through which the fetal growth limitation might occur [7]. Moreover, in adults, increased DNL has been identified as an adaptive hepatic response to unlimited nutrient availability subsequent to prenatal caloric restrictions, a phenomenon associated to a rise in hepatic GLUT1 expression [60], which could potentially disrupt the regulation of glucose homeostasis. Hence, PTE-dependent metabolic alterations in the liver might relate to these mechanisms. Nevertheless, future research is warranted to assess which possible scenario(s) occurs. The characterization of PTE-induced metabolic changes is pivotal for future research aiming to design nutritional approaches that can regulate liver DNL, to maintain steady blood glucose levels, and to restore brain glucose metabolism. Such understanding will aid in deciphering whether PTE-induced changes in liver metabolism contribute to, or depend on, the onset of psychiatric disorders.

We acknowledge that while our study provides insights into the metabolic changes induced by PTE, the direct application of these findings to clinical settings requires a rigorous validation in human studies. Should future research confirm that the metabolic and microbiota alterations observed in our study are indeed associated with psychiatric disorders in humans, this would underscore the potential of targeted nutritional strategies as a novel intervention for PTE-dependent deleterious effects. Such strategies could be designed to ameliorate metabolic and microbiota imbalances, with the ultimate goal of evaluating their impact on the psychiatric disorders associated with PTE. This approach not only promises to advance our understanding of the metabolic underpinnings of psychiatric conditions but also opens avenues for developing preventive and therapeutic strategies that address the metabolic component of these disorders.

Funding source

This research was funded by grants to GC and SB from the University of Cagliari: Fondo Integrativo per la Ricerca (FIR 2019) and by the FISR 2019-00202 DIETAMI (M.M). The supporting source had no involvement or restrictions regarding publication.

CRediT authorship contribution statement

Elisabetta Murru: Writing – review & editing, Writing – original draft, Methodology, Investigation, Formal analysis, Data curation, Conceptualization. **Gianfranca Carta:** Writing – review & editing, Writing – original draft, Methodology, Investigation, Funding acquisition, Formal analysis, Data curation, Conceptualization. **Claudia Manca:** Writing – review & editing, Writing – original draft, Methodology, Investigation, Formal analysis, Data curation, Conceptualization. **Marko Verce:** Writing – review & editing, Writing – original draft, Methodology, Investigation, Formal analysis, Data curation. **Amandine Everard:** Writing – review & editing, Writing – original draft, Methodology, Investigation, Formal analysis, Data curation. **Valeria Serra:** Writing – review & editing, Writing – original draft, Methodology, Investigation, Formal analysis. **Sonia Aroni:** Writing – review & editing, Writing – original draft, Methodology, Investigation, Formal analysis. **Miriam Melis:** Writing – review & editing, Writing – original draft, Supervision, Investigation, Funding acquisition, Data curation, Conceptualization. **Sebastiano Banni:** Writing – review & editing, Writing – original draft, Supervision, Investigation, Funding acquisition, Data curation, Conceptualization.

Declaration of competing interest

The authors declare that they have no known competing financial interests or personal relationships that could have appeared to

influence the work reported in this paper.

Acknowledgements

We acknowledge the CeSAR (Centro Servizi Ricerca d'Ateneo) core facility of the University of Cagliari and Dr. Marta Costa for assistance with the generation of 16S rRNA gene sequencing.

References

[1] A. Petrangelo, N. Czuzoj-Shulman, J. Balayla, H.A. Abenhaim, Cannabis abuse or dependence during pregnancy: a population-based cohort study on 12 million births, J. Obstet. Gynaecol. Can. 41 (5) (2019) 623–630.
[2] R.A. Brown, H. Dakkak, J. Gilliland, J.A. Seabrook, Predictors of drug use during pregnancy: the relative effects of socioeconomic, demographic, and mental health risk factors, J. Neonatal Perinat. Med. 12 (2) (2019) 179–187.
[3] C. Roncero, I. Valriberas-Herrero, M. Mezzatesta-Gava, J.L. Villegas, L. Aguilar, L. Grau-Lopez, Cannabis use during pregnancy and its relationship with fetal developmental outcomes and psychiatric disorders. A systematic review, Reprod. Health 17 (1) (2020) 25.
[4] D.J. Corsi, J. Donelle, E. Sucha, S. Hawken, H. Hsu, D. El-Chaar, et al., Maternal cannabis use in pregnancy and child neurodevelopmental outcomes, Nat. Med. 26 (10) (2020) 1536–1540.
[5] S. Patel, S. Khan, S. M, P. Hamid, The association between cannabis use and schizophrenia: causative or curative? A systematic review, Cureus 12 (7) (2020) e9309.
[6] X. Chang, Y. Bian, Q. He, J. Yao, J. Zhu, J. Wu, et al., Suppression of STAT3 signaling by delta9-tetrahydrocannabinol (THC) induces trophoblast dysfunction, Cell. Physiol. Biochem. 42 (2) (2017) 537–550.
[7] B.V. Natale, K.N. Gustin, K. Lee, A.C. Holloway, S.R. Laviolette, D.R.C. Natale, et al., Delta9-tetrahydrocannabinol exposure during rat pregnancy leads to symmetrical fetal growth restriction and labyrinth-specific vascular defects in the placenta, Sci. Rep. 10 (1) (2020) 544.
[8] M.G. Nashed, D.B. Hardy, S.R. Laviolette, Prenatal cannabinoid exposure: emerging evidence of physiological and neuropsychiatric abnormalities, Front. Psychiatr. 11 (2020) 624275.
[9] H. El Marroun, H. Tiemeier, E.A. Steegers, V.W. Jaddoe, A. Hofman, F.C. Verhulst, et al., Intrauterine cannabis exposure affects fetal growth trajectories: the Generation R Study, J. Am. Acad. Child Adolesc. Psychiatry 48 (12) (2009) 1173–1181.
[10] M.H. Sarikahya, S. Cousineau, M. De Felice, K. Lee, K.K. Wong, M.V. DeVuono, et al., Prenatal THC exposure induces sex-dependent neuropsychiatric endophenotypes in offspring and long-term disruptions in fatty-acid signaling pathways directly in the mesolimbic circuitry, eNeuro 9 (5) (2022).
[11] B.F. Moore, K.A. Sauder, A.L.B. Shapiro, T. Crume, G.L. Kinney, D. Dabelea, Fetal exposure to cannabis and childhood metabolic outcomes: the healthy start study, J. Clin. Endocrinol. Metab. 107 (7) (2022) e2862–e2869.
[12] T. Jourdan, G. Godlewski, G. Kunos, Endocannabinoid regulation of beta-cell functions: implications for glycaemic control and diabetes, Diabetes Obes. Metabol. 18 (6) (2016) 549–557.
[13] S.J. Wakil, L.A. Abu-Elheiga, Fatty acid metabolism: target for metabolic syndrome, J. Lipid Res. 50 (Suppl) (2009) S138–S143. Suppl.
[14] C.K. Glass, J.M. Olefsky, Inflammation and lipid signaling in the etiology of insulin resistance, Cell Metabol. 15 (5) (2012) 635–645.
[15] E. Cross, D.J. Dearlove, L. Hodson, Nutritional regulation of hepatic de novo lipogenesis in humans, Curr. Opin. Clin. Nutr. Metab. Care 26 (2) (2023) 65–71.
[16] M. Yilmaz, K.C. Claiborn, G.S. Hotamisligil, De novo lipogenesis products and endogenous lipokines, Diabetes 65 (7) (2016) 1800–1807.
[17] D. Osei-Hyiaman, M. DePetrillo, P. Pacher, J. Liu, S. Radaeva, S. Batkai, et al., Endocannabinoid activation at hepatic CB1 receptors stimulates fatty acid synthesis and contributes to diet-induced obesity, J. Clin. Invest. 115 (5) (2005) 1298–1305.
[18] P.D. Cani, H. Plovier, M. Van Hul, L. Geurts, N.M. Delzenne, C. Druart, et al., Endocannabinoids–at the crossroads between the gut microbiota and host metabolism, Nat. Rev. Endocrinol. 12 (3) (2016) 133–143.
[19] E. Murru, P.A. Lopes, G. Carta, C. Manca, A. Abolghasemi, J.L. Guil-Guerrero, et al., Different dietary N-3 polyunsaturated fatty acid formulations distinctively modify tissue fatty acid and N-acylethanolamine profiles, Nutrients 13 (2) (2021).
[20] I. Matias, G. Carta, E. Murru, S. Petrosino, S. Banni, V. Di Marzo, Effect of polyunsaturated fatty acids on endocannabinoid and N-acyl-ethanolamine levels in mouse adipocytes, Biochim. Biophys. Acta 1781 (1–2) (2008) 52–60.
[21] S. Banni, V. Di Marzo, Effect of dietary fat on endocannabinoids and related mediators: consequences on energy homeostasis, inflammation and mood, Mol. Nutr. Food Res. 54 (1) (2010) 82–92.
[22] S.S. Naughton, M.L. Mathai, D.H. Hryciw, A.J. McAinch, Fatty Acid modulation of the endocannabinoid system and the effect on food intake and metabolism, Internet J. Endocrinol. 2013 (2013) 361895.
[23] K. Tsuboi, T. Uyama, Y. Okamoto, N. Ueda, Endocannabinoids and related N-acylethanolamines: biological activities and metabolism, Inflamm. Regen. 38 (2018) 28.
[24] M.V. Chakravarthy, Z. Pan, Y. Zhu, K. Tordjman, J.G. Schneider, T. Coleman, et al., "New" hepatic fat activates PPARalpha to maintain glucose, lipid, and cholesterol homeostasis, Cell Metabol. 1 (5) (2005) 309–322.
[25] P.D. Cani, M. Van Hul, C. Lefort, C. Depommier, M. Rastelli, A. Everard, Microbial regulation of organismal energy homeostasis, Nat. Metab. 1 (1) (2019) 34–46.
[26] Z. Mehmedic, S. Chandra, D. Slade, H. Denham, S. Foster, A.S. Patel, et al., Potency trends of Delta9-THC and other cannabinoids in confiscated cannabis preparations from 1993 to 2008, J. Forensic Sci. 55 (5) (2010) 1209–1217.
[27] R. Frau, V. Miczan, F. Traccis, S. Aroni, C.I. Pongor, P. Saba, et al., Prenatal THC exposure produces a hyperdopaminergic phenotype rescued by pregnenolone, Nat. Neurosci. 22 (12) (2019) 1975–1985.
[28] J. Huber, S. Darling, K. Park, K.F. Soliman, Altered responsiveness to stress and NMDA following prenatal exposure to cocaine, Physiol. Behav. 72 (1–2) (2001) 181–188.
[29] M.P. Melis, E. Angioni, G. Carta, E. Murru, P. Scanu, S. Spada, et al., Characterization of conjugated linoleic acid and its metabolites by RP-HPLC with diode array detector, Eur. J. Lipid Sci. Technol. 103 (9) (2001) 617–621.
[30] S.D. Chiang, C.F. Gessert, O.H. Lowry, Colorimetric determination of extracted lipids, An adaptation for microgram amounts of lipids obtained from cerumen 33 (1957) 56.
[31] S. Banni, G. Carta, M.S. Contini, E. Angioni, M. Deiana, M.A. Dessì, et al., Characterization of conjugated diene fatty acids in milk, dairy products, and lamb tissues, J. Nutr. Biochem. 7 (3) (1996) 150–155.
[32] B. Batetta, M. Griinari, G. Carta, E. Murru, A. Ligresti, L. Cordeddu, et al., Endocannabinoids may mediate the ability of (n-3) fatty acids to reduce ectopic fat and inflammatory mediators in obese zucker rats, J. Nutr. 139 (8) (2009) 1495–1501.
[33] C. Quast, E. Pruesse, P. Yilmaz, J. Gerken, T. Schweer, P. Yarza, et al., The SILVA ribosomal RNA gene database project: improved data processing and web-based tools, Nucleic Acids Res. 41 (Database issue) (2013) D590–D596.
[34] E. Bolyen, J.R. Rideout, M.R. Dillon, N.A. Bokulich, C.C. Abnet, G.A. Al-Ghalith, et al., Reproducible, interactive, scalable and extensible microbiome data science using QIIME 2, Nat. Biotechnol. 37 (8) (2019) 852–857.
[35] M. Martin, Cutadapt removes adapter sequences from high-throughput sequencing reads, EMBnet Journal 17 (2011) 10–12.
[36] B.J. Callahan, P.J. McMurdie, M.J. Rosen, A.W. Han, A.J. Johnson, S.P. Holmes, DADA2: high-resolution sample inference from Illumina amplicon data, Nat. Methods 13 (7) (2016) 581–583.
[37] M.S. Robeson, D.R. O'Rourke, B.D. Kaehler, M. Ziemski, M.R. Dillon, J.T. Foster, et al., RESCRIPt: reproducible sequence taxonomy reference database management, PLoS Comput. Biol. 17 (11) (2021) e1009581.

[38] C. Lozupone, R. Knight, UniFrac: a new phylogenetic method for comparing microbial communities, Appl. Environ. Microbiol. 71 (12) (2005) 8228–8235.
[39] S. Mandal, W. Van Treuren, R.A. White, M. Eggesbo, R. Knight, S.D. Peddada, Analysis of composition of microbiomes: a novel method for studying microbial composition, Microb. Ecol. Health Dis. 26 (2015) 27663.
[40] F.W. Sanders, J.L. Griffin, De novo lipogenesis in the liver in health and disease: more than just a shunting yard for glucose, Biol. Rev. Camb. Phil. Soc. 91 (2) (2016) 452–468.
[41] E. Murru, P.A. Lopes, G. Carta, C. Manca, A. Abolghasemi, J.L. Guil-Guerrero, et al., Different dietary n-3 polyunsaturated fatty acid formulations distinctively modify tissue fatty acid and n-acylethanolamine profiles, Nutrients 13 (2) (2021) 1–16.
[42] B. Batetta, M. Griinari, G. Carta, E. Murru, A. Ligresti, L. Cordeddu, et al., Endocannabinoids may mediate the ability of (n-3) fatty acids to reduce ectopic fat and inflammatory mediators in obese Zucker rats, J. Nutr. 139 (8) (2009) 1495–1501.
[43] R. Crescenzo, A. Mazzoli, R. Cancelliere, F. Bianco, A. Giacco, G. Liverini, et al., Polyunsaturated fatty acids stimulate de novo lipogenesis and improve glucose homeostasis during refeeding with high fat diet, Front. Physiol. 8 (2017) 178.
[44] S.E. O'Sullivan, A.S. Yates, R.K. Porter, The peripheral cannabinoid receptor type 1 (CB(1)) as a molecular target for modulating body weight in man, Molecules 26 (20) (2021).
[45] M. Melis, G. Carta, M. Pistis, S. Banni, Physiological role of peroxisome proliferator-activated receptors type alpha on dopamine systems, CNS Neurol. Disord.: Drug Targets 12 (1) (2013) 70–77.
[46] S. Vernia, J. Cavanagh-Kyros, L. Garcia-Haro, G. Sabio, T. Barrett, D.Y. Jung, et al., The PPARalpha-FGF21 hormone axis contributes to metabolic regulation by the hepatic JNK signaling pathway, Cell Metabol. 20 (3) (2014) 512–525.
[47] J. Iglesias, L. Morales, G.E. Barreto, Metabolic and inflammatory adaptation of reactive astrocytes: role of PPARs, Mol. Neurobiol. 54 (4) (2017) 2518–2538.
[48] P. Steiner, Brain fuel utilization in the developing brain, Ann. Nutr. Metab. 75 (Suppl 1) (2019) 8–18.
[49] M. Knobloch, S.M. Braun, L. Zurkirchen, C. von Schoultz, N. Zamboni, M.J. Arauzo-Bravo, et al., Metabolic control of adult neural stem cell activity by Fasn-dependent lipogenesis, Nature 493 (7431) (2013) 226–230.
[50] T. Harayama, H. Riezman, Understanding the diversity of membrane lipid composition, Nat. Rev. Mol. Cell Biol. 19 (5) (2018) 281–296.
[51] N.L. Cluny, C.M. Keenan, R.A. Reimer, B. Le Foll, K.A. Sharkey, Prevention of diet-induced obesity effects on body weight and gut microbiota in mice treated chronically with delta9-tetrahydrocannabinol, PLoS One 10 (12) (2015) e0144270.
[52] L.M. Cox, J. Sohn, K.L. Tyrrell, D.M. Citron, P.A. Lawson, N.B. Patel, et al., Description of two novel members of the family Erysipelotrichaceae: Ileibacterium valens gen. nov., sp. nov. and Dubosiella newyorkensis, gen. nov., sp. nov., from the murine intestine, and emendation to the description of Faecalibaculum rodentium, Int. J. Syst. Evol. Microbiol. 67 (5) (2017) 1247–1254.
[53] Q. Zhu, Y. Zhu, Y. Liu, Y. Tao, Y. Lin, S. Lai, et al., Moderation of gut microbiota and bile acid metabolism by chlorogenic acid improves high-fructose-induced salt-sensitive hypertension in mice, Food Funct. 13 (13) (2022) 6987–6999.
[54] D.J. Fernandes, S. Spring, A.R. Roy, L.R. Qiu, Y. Yee, B.J. Nieman, et al., Exposure to maternal high-fat diet induces extensive changes in the brain of adult offspring, Transl. Psychiatry 11 (1) (2021) 149.
[55] J.J. Chen, P. Zheng, Y.Y. Liu, X.G. Zhong, H.Y. Wang, Y.J. Guo, et al., Sex differences in gut microbiota in patients with major depressive disorder, Neuropsychiatric Dis. Treat. 14 (2018) 647–655.
[56] M.I. Butler, T.F.S. Bastiaanssen, C. Long-Smith, S. Morkl, K. Berding, N.L. Ritz, et al., The gut microbiome in social anxiety disorder: evidence of altered composition and function, Transl. Psychiatry 13 (1) (2023) 95.
[57] M.V. Selma, D. Beltran, R. Garcia-Villalba, J.C. Espin, F.A. Tomas-Barberan, Description of urolithin production capacity from ellagic acid of two human intestinal Gordonibacter species, Food Funct. 5 (8) (2014) 1779–1784.
[58] M. Kujawska, J. Jodynis-Liebert, Polyphenols in Parkinson's disease: a systematic review of in vivo studies, Nutrients 10 (5) (2018).
[59] X. Liu, B. Mao, J. Gu, J. Wu, S. Cui, G. Wang, et al., Blautia-a new functional genus with potential probiotic properties? Gut Microb. 13 (1) (2021) 1–21.
[60] M. Garg, M. Thamotharan, Y. Dai, V. Lagishetty, A.V. Matveyenko, W.N. Lee, et al., Glucose intolerance and lipid metabolic adaptations in response to intrauterine and postnatal calorie restriction in male adult rats, Endocrinology 154 (1) (2013) 102–113.